fortune Journals

Research Article

CARDIOLOGY AND CARDIOVASCULAR MEDICINE

ISSN: 2572-9292

Unveiling the Cardioprotective Potential of HY-021068: Dual Modulation of Calcium Homeostasis and Endoplasmic Reticulum Stress in Myocardial Infarction in Mice

Yuqing Chu[1], Xinya Wang[1,2+], Hongyan Zhang[1], Shihao Wan[1], Qiuju Zhao[1], Yani Guo[1], Ke Niu[2], Binshan Zha[3], Jiajia Mo[4,5], Qichao Luo[1], Zhaoxing Chu[4], Liwen Chen[2*], Liuyi Dong[1,2*]

Abstract

Acute myocardial infarction (AMI) remains a leading cause of death worldwide and is characterized by abrupt coronary occlusion and subsequent ischemic cardiomyocyte injury. Increasing evidence implicates endoplasmic reticulum (ER) stress and disordered calcium handling as central drivers of post-infarction dysfunction. Here, we investigated whether HY-021068 (HY), a thromboxane synthase inhibitor under clinical evaluation, confers cardioprotection by restoring sarco/endoplasmic reticulum Ca^{2+}-ATPase 2a (SERCA2a)-dependent calcium homeostasis and suppressing ER stress. AMI was induced in C57BL/6 mice by left anterior descending coronary artery ligation, and an oxygen–glucose deprivation/reperfusion (OGD/R) model was established in AC16 cardiomyocytes. Infarct size and tissue injury were assessed by TTC staining, H&E and Masson staining, and cardiac function was quantified by echocardiography. Intracellular reactive oxygen species (ROS) and Ca^{2+} levels were measured using DCFH-DA and Fluo-4 AM, respectively. Mitochondrial ultrastructure and function were evaluated by transmission electron microscopy, JC-1 membrane potential assays, and ATP quantification. Key proteins involved in calcium cycling, ER stress, and thromboxane signaling were analyzed by immunoblotting and immunostaining.HY treatment reduced infarct size, attenuated myocardial fibrosis, and improved left ventricular systolic function. In vitro, HY decreased OGD/R-induced cytosolic Ca^{2+} overload, lowered ROS accumulation, and restored mitochondrial membrane potential and ATP production. Mechanistically, HY increased SERCA2a expression and shifted the calcium-handling program toward SR Ca^{2+} reuptake, accompanied by reduced expression of IP3R and NCX-1 and suppression of ER stress markers (GRP78, ATF6, and CHOP). Consistent with its pharmacological class, HY inhibited platelet aggregation and modulated thromboxane-related proteins, including COX-1, TBXAS-1, and PGD.Collectively, these data indicate that HY exerts cardioprotective effects in AMI by dual modulation of calcium homeostasis and ER stress, with SERCA2a as a key molecular node. HY therefore represents a promising multi-target candidate for ischemic heart disease.

Keywords: HY-021068; Myocardial infarction; SERCA2a; Endoplasmic reticulum stress

Introduction

Acute myocardial infarction (AMI) is typified by mocardium necrosis ensuing from acute ischemia and hypoxia within the coronary arteries. In severe scenarios, it may precipitate heart failure [1]. By 2019, the global prevalence

Affiliation:

[1]Department of Pharmacology, Key Laboratory of Anti-Inflammatory and Immunopharmacology of Ministry of Education, Key Laboratory of Chinese Medicine Research and Development of State Administration of Traditional Chinese Medicine, School of Pharmacy, Anhui Medical University, Hefei, Anhui, China

[2]Research Center for Translational Medicine, Department of Blood Transfusion, The Second Affiliated Hospital of Anhui Medical University, Hefei, Anhui, China

[3]Department of Vascular and Thyroid Surgery, Department of General Surgery, The First Affiliated Hospital of Anhui Medical University, Hefei, Anhui, China

[4]Hefei Industrial and Pharmaceutical Industry Co., Ltd, Hefei, Anhui, China

[5]School of Pharmacy, China Pharmaceutical University, Nanjing, Jiangsu, China

***Corresponding author:**

Liuyi Dong, Department of Pharmacology, Key Laboratory of Anti-Inflammatory and Immunopharmacology of Ministry of Education, Key Laboratory of Chinese Medicine Research and Development of State Administration of Traditional Chinese Medicine, School of Pharmacy, Anhui Medical University, Hefei, Anhui, China.

Liwen Chen, Research Center for Translational Medicine, Department of Blood Transfusion, The Second Affiliated Hospital of Anhui Medical University, Hefei, Anhui, China

+Yuqing Chu, Xinya Wang contributed equally to this work.

Citation: Yuqing Chu, Xinya Wang, Hongyan Zhang, Shihao Wan, Qiuju Zhao, Yani Guo, Ke Niu, Binshan Zha, Jiajia Mo, Qichao Luo, Zhaoxing Chu, Liwen Chen, Liuyi Dong. Unveiling the Cardioprotective Potential of HY-021068: Dual Modulation of Calcium Homeostasis and Endoplasmic Reticulum Stress in Myocardial Infarction in Mice. Cardiology and Cardiovascular Medicine. 10 (2026): 127-144.

Received: February 06, 2026
Accepted: February 20, 2026
Published: May 26, 2026

of cardiovascular diseases (CVD) had reached 523 million, with 18.6 million annual deaths. According to Markov model projections, between 2010 and 2030, China is projected to experience 21.3 million new cardiovascular events and 7.7 million cardiovascular-related deaths [2]. CVD have emerged as the predominant cause of mortality in both urban and rural Chinese populations, with 40% of deaths attributable to cardiovascular incidents [3,4]. As a critical and life-threatening condition within the broader spectrum of CVD, the incidence of AMI has been increasing annually, emerging as a predominant factor contributing to global mortality and morbidity. Nevertheless, the exact pathophysiological mechanisms implicated in AMI still lack comprehensive understanding, and effective therapeutic strategies have yet to be established [5]. Despite major advances in reperfusion and secondary prevention, AMI continues to impose a substantial global health burden, and many patients progress to heart failure because myocardial injury and remodeling are not fully prevented. A deeper mechanistic understanding of injury amplification pathways that operate during and after ischemia is therefore essential for the development of adjunctive cardioprotective therapies. Existing research indicates that the abnormal elevation of calcium ions, a condition known as calcium overload, is a major cause of myocardial injury following AMI [6-8]. Therefore, drugs that alleviate calcium overload are considered potential therapeutic agents for the treatment of myocardial infarction.

Calcium overload occurs when various harmful factors disrupt the calcium homeostasis mechanism, leading to abnormal distribution of calcium ions and elevated intracellular calcium concentrations [9-13]. In 1966, Zimmerman and Hulsmann demonstrated that perfusion of isolated rat hearts with calcium-free saline caused membrane damage within a short time frame [14]. Subsequent perfusion with normal calcium-containing saline resulted in more pronounced structural and functional changes in the heart. Recent studies have shown significant alterations in calcium regulation during myocardial infarction (M/I) development, and restoring or maintaining calcium homeostasis has been shown to reduce cellular damage and limit necrosis [15-17]. Furthermore, inhibiting calcium overload can protect damaged mitochondria, reduce oxidative stress, and attenuate inflammation, thereby exerting a protective effect in myocardial infarction. Therefore, investigating the role and underlying mechanisms of calcium overload in AMI is crucial [18]. Therapeutic strategies that stabilize Ca^{2+} handling are therefore expected to limit injury and improve functional recovery.

The sarco/endoplasmic reticulum Ca^{2+}-ATPase 2a (SERCA2a) represents a pivotal proteinaceous entity responsible for re-uptaking cytosolic calcium ions and transporting them into the sarcoplasmic reticulum (SR), thereby facilitating myocardial cell relaxation. The SR Ca^{2+} pump sarco/endoplasmic reticulum Ca^{2+}-ATPase 2a (SERCA2a) is a central determinant of cardiac Ca^{2+} cycling because it clears cytosolic Ca^{2+} and reloads the SR to enable both relaxation and subsequent contraction. Reduced SERCA2a expression and/or activity has been documented in ischemic and failing myocardium and is associated with impaired SR Ca^{2+} reuptake, diastolic Ca^{2+} leak, and reduced contractile reserve [19-22]. Importantly, SERCA2a dysfunction also intersects with endoplasmic reticulum (ER) stress. The ER/SR is a major intracellular Ca^{2+} store, and depletion of luminal Ca^{2+} compromises protein folding capacity and triggers the unfolded protein response. While adaptive ER stress responses can be protective, sustained activation of pro-death ER stress signaling (e.g., GRP78–ATF6 and CHOP) contributes to cardiomyocyte loss and maladaptive remodeling. Agents that enhance SERCA2a activity may therefore provide dual benefit by correcting Ca^{2+} mishandling and relieving ER stress.Reduced expression and activity of SERCA2a disrupt calcium homeostasis in cardiomyocytes, a hallmark feature of myocardial infarction [23-25]. From recent research, enhancing SERCA2a function can lessen ER stress, restore mitochondrial function, and relieve cardiac calcium overload [26]. Consequently, augmenting the involvement of SERCA2a activity is crucial in the therapeutic intervention for patients afflicted with AMI.

HY-021068 (HY), a thromboxane synthase inhibitor, has been demonstrated by extant studies to alleviate the symptoms of cerebral infarction [27]. It achieves this through specific mechanisms: inhibiting the synthesis of thromboxane A2 (TXA2), thereby impeding platelet aggregation, as well as exerting anti-inflammatory and neuroprotective functions [28]. Our preliminary assessment suggests that HY-021068, presently under clinical trials, exhibits potent antiplatelet aggregation and ischemia-reperfusion protection capabilities. These research findings indicate that HY exhibits potential as a novel therapeutic agent for AMI as reported by Li et al. [29]. Nevertheless, the exact molecular and cellular mechanisms mediating its pharmacological action remain elusive. In this work, we hypothesize that HY may enhance SERCA2a function, hence alleviating calcium overload-induced ER stress and mitochondrial dysfunction in myocardial infarction. SERCA2a, a key regulator of intracellular calcium, is crucial for cellular homeostasis [30]. Its dysfunction during infarction disrupts calcium handling, leading to ER stress and mitochondrial problems [31]. HY may act to correct this and mitigate pathological consequences. Our findings could provide novel strategies for the treatment of AMI.

In this study, we tested the hypothesis that HY protects the ischemic heart by restoring SERCA2a-dependent Ca^{2+} homeostasis and suppressing Ca^{2+}-driven ER stress and mitochondrial dysfunction. Using a mouse model of AMI induced by left anterior descending coronary artery ligation and an OGD/R model in AC16 cardiomyocytes, we assessed

Chu Y, et al., Cardiol Cardiovasc Med 2026
DOI:10.26502/fccm.92920492

functional and histological outcomes and interrogated the molecular pathways linking SERCA2a, Ca^{2+} cycling, ER stress, and mitochondrial energetics. Our findings provide mechanistic evidence that HY exerts cardioprotection through coordinated regulation of Ca^{2+} homeostasis and ER stress.

Materials and Methods

Animals

Eight-week-old male C57BL/6 mice (20-25 g, SPF grade) were obtained from Zhejiang Ziyuan Laboratory Animal Technology Co. (Hangzhou, China). Animals were housed under controlled conditions (22-24°C, 12-h light/dark cycle) with ad libitum access to food and water. All procedures were approved by the Animal Ethics Committee of Anhui Medical University (SYXK(WAN)2017-006). One hundred twenty mice were randomly divided into six groups (n=20/group). Namely, there was a control group and a model group (administered with saline), three HY treatment groups (12.5, 25, and 50 mg/kg), and a clopidogrel intervention group (15 mg/kg). By binding the left anterior descending (LAD) coronary artery, AMI formed in the mice [32-34]. The mice were administered the corresponding drugs at loading doses continuously for seven days. The daily dosage volume was precisely 0.2 ml per 100 g of body weight.

Establishment of AMI model

Mice were anesthetized with intraperitoneal 1.2% tribromoethanol (0.2 ml/10 g). Physiological stability was maintained using mechanical ventilation. Following ECG lead attachment to monitor cardiac activity, a fourth intercostal space thoracotomy exposed the heart. The LAD coronary artery was ligated (sham group underwent thoracotomy only without ligation). Successful ischemia was confirmed by ST-segment elevation, peaked T waves, QRS complex widening, and left ventricular wall blanching. Seven days post-MI, mice were euthanized by cervical dislocation for heart weight measurement and heart-to-body weight ratio calculation.

Measurement of infarct size

Seven days after LAD-induced myocardial infarction, the hearts of the mice were excised and immediately placed in a freezer. Distal to the ligation site, the heart tissue was cut into 1-mm thick transverse sections and then placed in a solution consisting of 1% of 2,3,5-triphenyltetrazolium chloride (TTC, Sigma, USA) [35-37]. Samples were incubated at 37°C for 30 minutes. Following staining, viable myocardium appeared red and infarcted areas white. After that, tissues were preserved histologically by putting to 4% paraformaldehyde (PFA). Infarct area quantification was performed using ImageJ software by blinded independent investigators.

Echocardiography

At the end of the treatment, echocardiographic assessment was performed. Images were acquired using the VINNO 6 Vet portable Doppler ultrasound system, and M-mode was used to measure cardiac function. The acquired data was utilized to compute the Left Ventricular Ejection Fraction (LVEF) and the Left Ventricular Fractional Shortening (LVFS).

Histological examination

The murine hearts were initially fixed with 4% paraformaldehyde solution, followed by a dehydration process using a series of graded ethanol concentrations, and then cleared with xylene to enhance tissue transparency. Subsequently, the heart tissue was embedded in paraffin wax for stabilization and sectioned into slices with a thickness of precisely 5 mm. These histological sections were subjected to hematoxylin and eosin (H&E) staining to meticulously observe any pathological alterations. In addition, Masson's trichrome staining was applied to precisely gauge the amount of collagen released in the tissue [38].

Immunohistochemistry staining

Tissues fixed in paraffin were cut into 5 mm sections and put on slides. After deparaffinization and rehydration, sections were blocked with 5% goat serum/PBS containing 0.3% Triton X-100 for 1 h at room temperature to reduce nonspecific binding. Primary antibody against SERCA2a (1:300, Affinity) was applied overnight at 4°C. Following PBS washes, sections were incubated with secondary antibody (1 h, RT) and developed using DAB (ZSGB-BIO).

ELISA

Serum levels of 6-keto-PGF1α, TXB2, CK-MB, LDH and cTnI were quantified using a commercial ELISA kit (Jiangsu Enzyme Immunoassay). Following sample dilution, aliquots were added to antibody-coated 96-well plates. After incubation and washing, plates were sequentially incubated with biotinylated secondary antibody and streptavidin-HRP conjugate. Reactions were halted after the addition of substrate and color development, and absorbance was measured using a Bio-Rad microplate reader at 450 nm. Analyte concentrations (ng/ml) were calculated from standard curves.

Mouse platelet aggregation *in vitro*

$$PAI = \left(1 - \frac{\text{maximum aggregation rate (MAR) of NS-treated PRP}}{\text{MAR of sample-treated PRP}}\right) \times 100\%$$

Blood samples were collected from the carotid artery and instantaneously anticoagulated with sodium citrate in a volume ratio of 9:1. To obtain platelet-rich plasma (PRP), the blood samples underwent centrifugation at 120 g for exactly 10 minutes. Subsequently, once the platelet-rich plasma (PRP) had been isolated, the residual blood was subjected to further centrifugation at 1600 g for 10 minutes in order to obtain platelet-poor plasma (PPP). The obtained PRP was then incubated with one of the following: normal saline (NS), clopidogrel at a dose of 15 mg/kg, or HY at concentrations of 12.5, 25, and 50 mg/kg[39-41]. Following incubation, the

Chu Y, et al., Cardiol Cardiovasc Med 2026
DOI:10.26502/fccm.92920492

PRP was stimulated with an aggregating agent, adenosine diphosphate (ADP) at a concentration of 10 mm. Finally, the platelet aggregation inhibition rate (PAI) was calculated using the formula:

AC16 cell culture and oxygen glucose deprivation model

AC16 and 293T cells were maintained in DMEM/F12 medium (Gibco) supplemented with 10% FBS and 100 μg/ml penicillin-streptomycin at 37°C in 5% CO_2, with medium changes every 48 hours. For the oxygen-glucose deprivation/reperfusion (OGD/R) experiments, AC16 cells were phosphate-buffered saline (PBS)-washed and incubated in glucose/FBS-free DMEM/F12 under hypoxic conditions (95% N_2/5% CO_2) for 6 h at 37°C [42]. The medium was subsequently replaced with complete DMEM/F12, and the culture conditions were restored to 37°C with 95% O_2 and 5% CO_2 for 2 hours.

Reactive oxygen species (ROS) detection

The DCFH-DA fluorescent probe served to test the level of intracellular ROS. AC16 cells were incubated with 10 mm DCFH-DA at a precisely regulated temperature of 37 °C for 30 minutes. After incubation, the cells were washed using phosphate-buffered saline (PBS) to remove any surplus and unreacted DCFH-DA. An inverted fluorescence microscope (Axio Observer 3, Germany) and a high-content filter (ImageXpress MicroConfocal, USA) were then used to collect the fluorescent signals. A mean fluorescence intensity followed.

Ca^{2+} content detection

Intracellular Ca^{2+} levels were measured using 5 mm Fluo-4 AM (Beyutime, China) dissolved in Ca^{2+}/Mg^{2+}-free HBSS. AC16 cells were seeded in 24-well plates and incubated overnight in F12 medium supplemented with 0.2% fetal bovine serum. After removing the medium, the cells were incubated with Fluo-4 AM at 37 °C for 30 minutes, followed by three washes with PBS. Next, fluorescent microscopy and high-content screening were used to record the intensity of fluorescence.

For extracellular Ca^{2+}, a calcium assay kit (Nanjing Jiancheng) was used. Mouse serum and extracellular fluid samples were mixed with MTB reagent and an alkaline solution and incubated at a constant temperature for 5 minutes. A microplate reader was used to detect absorbance at 610 nm, and the standard formula was used to determine the Ca^{2+} concentrations.

Immunofluorescence staining

As outlined above, AC16 cells were treated with HY and subjected to OGD. The cells were subjected to fixation and permeabilization procedures in preparation for subsequent immunostaining. Following that, 5% BSA was used to inhibit the cells for two hours at 37°C. The cells were treated with the anti-SERCA2a primary antibody for the full night at 4°C. Subsequently, the cells were placed in an incubator and cultured with a fluorescence-conjugated anti-rabbit secondary antibody at 37°C for 1 hour. After that, the nuclei were stained using DAPI. Subsequently, fluorescence images were acquired through the use of a confocal laser scanning microscope.

Transmission electron microscopy (TEM)

HY-pretreated AC16 cells were fixed in 2.5% glutaraldehyde/0.1 M phosphate buffer (pH 7.4) to whole night at 4°C. After post-fixation with 1% OsO_4, samples were ethanol-dehydrated and Epon Araldite-embedded. Ultrathin sections (50 nm) were prepared using an ultramicrotome (Leica Ultracut E), double-stained with uranyl acetate/lead citrate, and examined by TEM (Hitachi H-7000).

Measurement of mitochondrial membrane potential (ΔΨ)

Mitochondrial membrane potential (ΔΨ) was assessed using the JC-1 kit (Beyutime, China). For 20 minutes, cells are taken at 37°C with 50 nM JC-1. Fluorescence intensity was recorded using high-content screening (ImageXpress MicroConfocal, USA) to visualize the samples.

Detection of ATP content

An adenosine triphosphate (ATP) test kit was used to assess the value of ATP in the cells. Cell suspensions were seeded into 6-well plates or other appropriate culture plates at a specific density. The plates were then incubated under standard culture conditions until the cells adhered and grew to an appropriate confluence. After inducing cells with OGD/R and treating them with HY, cell lysis buffer and ATP detection reagent were added for the reaction. Subsequently, the absorbance was measured at 610 nm using a microplate reader (Bio-Rad, USA).

Plasmid constructs and transfection

The Myc-tagged SERCA2a domain was overexpressed and subsequently cloned into the pcDNA3.1-mCherry vector, which was obtained from Qingke Biotech (Beijing, China).

Simulation of molecular dynamics and molecular docking

Molecular docking was performed to assess HY's binding affinity with IP3R, RYR2, and SERCA2a. Receptor structures (RCSB PDB) and HY (PubChem) were prepared in AutoDockTools by converting to PDBQT format, removing solvents/ligands, and adding hydrogens/Kollman charges. Docking simulations used AutoDock Vina, with results visualized in PyMol. The HY-SERCA2a complex was further analyzed through 100-ns MD simulations (Gromacs 2022.4, Amber99 force field) in an SPC water solvated system (1.2 nm periodic box) with PME for electrostatics. The system

was neutralized with Na+/Cl- ions using Monte Carlo placement. Following energy minimization (steepest descent, 50,000 steps, Fmax<1000 kJ/mol), three equilibration phases were performed: (1) NVT (310 K, 50,000 steps, 2 fs); (2) NPT (310 K, 1 atm, 50,000 steps, 2 fs); and (3) production MD (100 ns, 2 fs).

Western blot

Total protein was extracted from frozen heart tissue with the aid of a cold tissue grinder in ice-cold RIPA buffer (Beyotime Biotechnology, Shanghai). The protein level was analyzed by a BCA assay kit (Beyotime Biotechnology, Shanghai). Subsequently, exactly 20 μg aliquots of protein were separated by 10% SDS-PAGE and then transferred onto a PVDF membrane (Millipore, USA) to conduct immunoblotting analysis. The membrane was blocked with 5% non-fat milk in Tris-buffered saline with 0.05% (v/v) Tween 20 (TBST) at room temperature for 2 hours, followed by overnight incubation with primary antibodies for SERCA2a (1:500, Affinity, DF6240), RYR2 (1:500, Affinity, AF0015), IP3R (1:500, Affinity, DF3000), PGD (1:500, Affinity, DF3714), COX-1 (1:500, Affinity, AF7002), TBXAS-1 (1:1000, Affinity, DF6739), ATF6 (1:1000, Affinity, DF6009), GRP78 (1:1000, Affinity, AF5366), CHOP (1:1000, Affinity, AF6277), p-CREB (1:500, Affinity, AF3189), CREB (1:500, Affinity, AF6188) and β-actin (1:10,000, Affinity, AF7018). Subsequent to three consecutive 10-minute washes with TBST, the membrane was subjected to incubation for one hour at ambient temperature in the presence of secondary antibodies conjugated either to goat anti-mouse (dilution 1:10,000, ZSGB-BIO, ZB2305) or goat anti-rabbit (dilution 1:10,000, ZSGB-BIO, ZB-2301). The target protein bands were visualized using a ChemiDoc imaging system (Bio-Rad, USA) and quantified with Image J software (NIH, USA). Expression levels were determined by normalizing each target band to its corresponding β-actin band.

Statistical analysis

Data are presented as mean ± SEM/SD. Statistical analyses were performed using GraphPad Prism 8.0, with Student's t-test for pairwise comparisons and one-way ANOVA (Tukey's HSD or Fisher's LSD post hoc tests) for multiple comparisons. Normality was verified for parametric tests. A threshold as statistical significance was $p<0.05$.

Results

HY's protective features against OGD/R-induced injury in vitro

To directly evaluate the inhibitory effect of HY on myocardial infarction in vitro, we employed an OGD/R-induced AC16 cell model to investigate its cardioprotective activity. As HY's concentration rose to 160mm, arose minimal cytotoxicity compare to the control (Figure 1A). Within a non-toxic concentration range, HY effectively protected AC16 cells from OGD/R-induced injury, demonstrating the highest cell viability and the lowest cytotoxicity at 40 mm (Figure 1B). Furthermore, cytotoxicity was further assessed by the LDH release assay, and the results indicated that HY treatment did not result in an increase in cytotoxicity (Figure 1C).

HY inhibits Ca^{2+} cycling and ER stress in vitro

Abnormal increases in intracellular calcium, induced by various factors, lead to cellular dysfunction and metabolic structural abnormalities, and in severe cases, may cause cell death [43-45]. To understand how HY protects against myocardial injury in vitro, we examined its effects using AC16 cells. Our findings indicate that oxygen-glucose deprivation/reperfusion (OGD/R) significantly raises intracellular Ca^{2+} levels while lowering extracellular Ca^{2+}, resulting in calcium overload (Figure 1D, G). Treatment with HY markedly reduced this overload. The underlying mechanism appears to involve the regulation of calcium-handling proteins. HY increases the expression of SERCA2a and ryanodine receptor 2 (RYR2), which enhances the uptake of Ca^{2+} by the sarcoplasmic/endoplasmic reticulum (SR/ER). At the same time, it decreases the expression of the inositol trisphosphate receptor (IP3R) and sodium-calcium exchanger (NCX-1), thereby mitigating calcium overload (Figure 1E). Excess intracellular Ca^{2+} disrupts ionic balance and the redox state, leading to excessive reactive oxygen species (ROS) production and oxidative stress. This process also stresses the endoplasmic reticulum, causing protein misfolding and, in severe cases, cell death. Consistent with these effects, we observed that OGD/R significantly hindered ATP production and increased ROS levels (Figure 1H, I). In addition, OGD/R activated glucose-regulated protein (GRP78), activating transcription factor 6 (ATF6), and C/EBP homologous protein (CHOP), three key endoplasmic reticulum stress markers. Notably, HY treatment significantly reduced the expression of these proteins (Figure 1J, K). In summary, HY exhibits a protective effect against OGD/R-induced myocardial injury, primarily mediated by reducing calcium overload, alleviating endoplasmic reticulum stress, and inhibiting pro-apoptotic pathways.

HY exhibits synergistic inhibitory effect with BAPTA-AM in vitro

BAPTA-AM (BA) is a selective calcium chelator that protects cells by alleviating intracellular Ca^{2+} overload [46, 47]. To validate our hypothesis that HY exerts its protective effect in vitro through the regulation of $[Ca^{2+}]$ i, we investigated its impact on OGD/R-induced myocardial injury. Our findings demonstrate that HY can correct the abnormal calcium cycling in myocardial cells caused by OGD/R, reduce the levels of ROS, increase the synthesis of ATP, alleviate

Chu Y, et al., Cardiol Cardiovasc Med 2026
DOI:10.26502/fccm.92920492

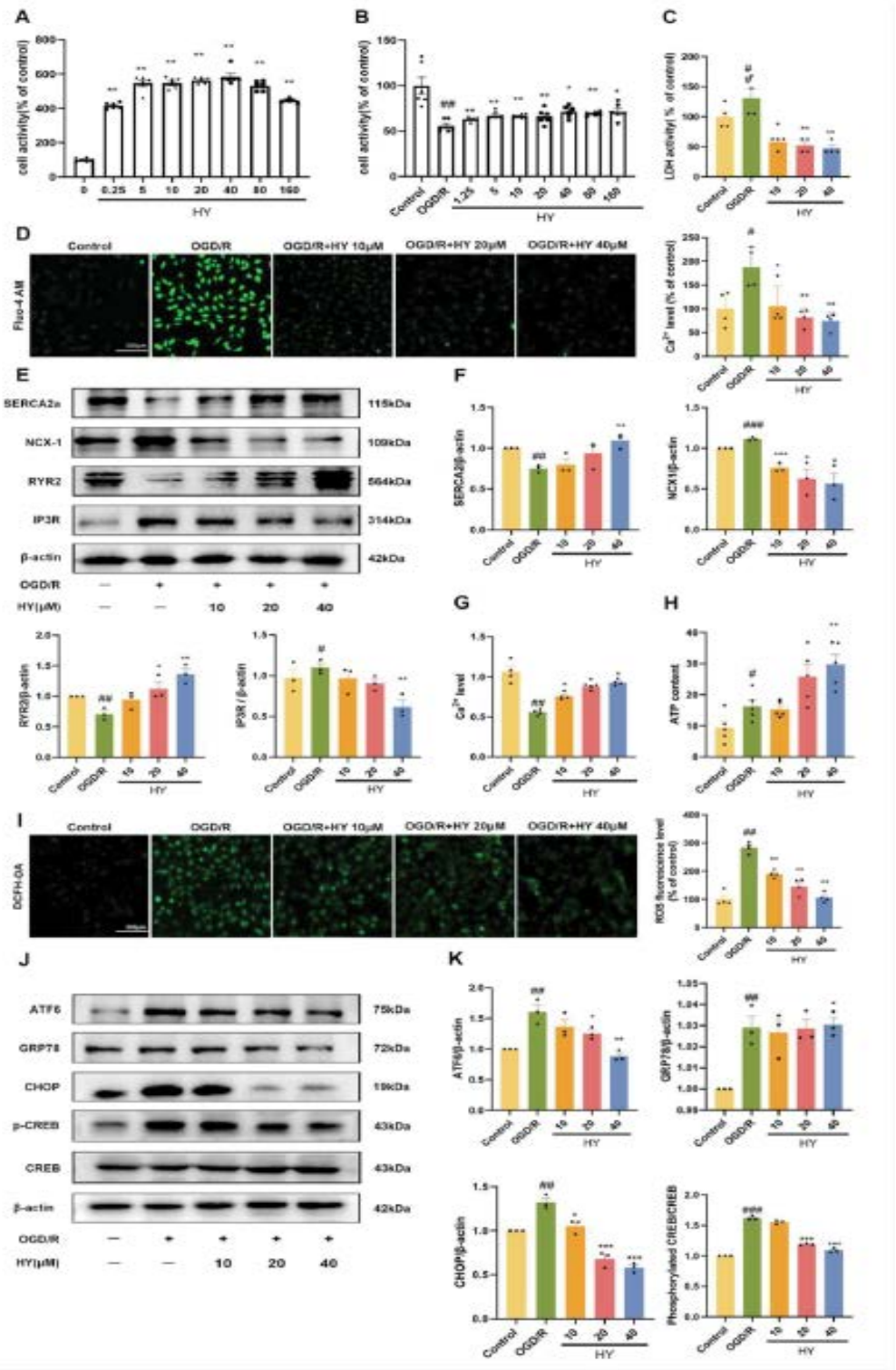

Figure 1: HY ameliorates the damage of AC16 cells induced by OGD/R. (A) Effects of different concentrations of HY on cell viability under normoxic conditions, n=6; (B) Effects of different concentrations of HY on cell viability under OGD/R conditions, n=6; (C) Effect of HY on LDH content in AC16 cell supernatant of OGD/R, n=4; (D) Intracellular Ca^{2+} fluorescence and quantification, scale bar 200 μm, n=6; (E-F) The expression of IP3R, RYR2, SERCA2a, and NCX-1 proteins, n=3; (G) Extracellular Ca^{2+} concentration changes, n=4; (H) ATP levels in OGD/R-injured cells with HY, n=5; (I) ROS fluorescence and quantification, scale bar 200 μm, n=4; (J-K) ER stress markers (ATF6, GRP78, CHOP) and CREB/p-CREB expression, n=3. $^{\#}P<0.05$ VS Control, $^{\#\#}P<0.01$ VS Control, $^{\#\#\#}P<0.001$ VS Control, $^{*}P<0.05$ VS OGD/R, $^{**}P<$VS OGD/R, $^{***}P<0.001$ VS OGD/R.

Citation: Yuqing Chu, Xinya Wang, Hongyan Zhang, Shihao Wan, Qiuju Zhao, Yani Guo, Ke Niu, Binshan Zha, Jiajia Mo, Qichao Luo, Zhaoxing Chu, Liwen Chen, Liuyi Dong. Unveiling the Cardioprotective Potential of HY-021068: Dual Modulation of Calcium Homeostasis and Endoplasmic Reticulum Stress in Myocardial Infarction in Mice. Cardiology and Cardiovascular Medicine.10 (2026): 127-144.

Chu Y, et al., Cardiol Cardiovasc Med 2026
DOI:10.26502/fccm.92920492

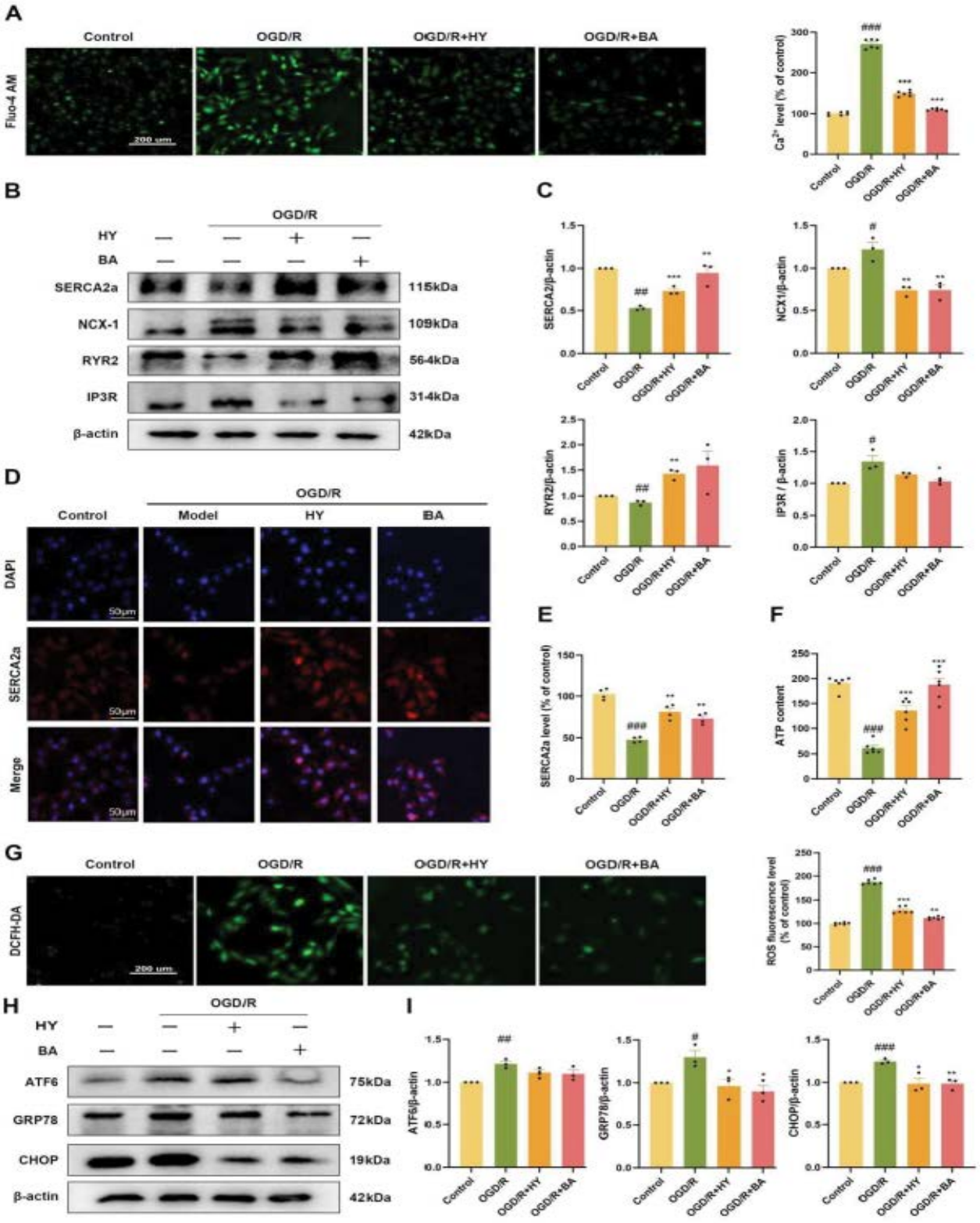

Figure 2: HY exhibits synergistic inhibitory effect with BA in vitro. (A) Intracellular Ca^{2+} levels, scale bar 200 μm, n=6; (B-C) Calcium channel protein expression (IP3R/RYR2/SERCA2a/NCX-1), n=3; (D-E) SERCA2a immunofluorescence and semi-quantitative analysis, scale bar 50 μm, n=4; (F) ATP concentration, n=6; (G) ROS fluorescence levels and analysis, scale bar 200 μm, n=6; (H) ER stress markers (ATF6, GRP78, CHOP) expression, n=3. $^{\#}$P<0.05 VS Control, $^{\#\#}$P<0.01 VS Control, ###P<0.001 VS Control, *P<0.05 VS OGD/R, **P<0.01 VS OGD/R, ***P<0.001 VS OGD/R.

Citation: Yuqing Chu, Xinya Wang, Hongyan Zhang, Shihao Wan, Qiuju Zhao, Yani Guo, Ke Niu, Binshan Zha, Jiajia Mo, Qichao Luo, Zhaoxing Chu, Liwen Chen, Liuyi Dong. Unveiling the Cardioprotective Potential of HY-021068: Dual Modulation of Calcium Homeostasis and Endoplasmic Reticulum Stress in Myocardial Infarction in Mice. Cardiology and Cardiovascular Medicine.10 (2026): 127-144.

Chu Y, et al., Cardiol Cardiovasc Med 2026
DOI:10.26502/fccm.92920492

endoplasmic ER, and its effects are comparable to those of BA (Figure 2A, F-G). The results of detecting the expression levels of calcium ion channels and ER stress-related proteins in myocardial cells show that both HY and BA upregulate the expressions of SERCA2a and RYR2, and simultaneously downregulate the expressions of IP3R, NCX-1, ATF6, GRP78, and CHOP. These two compounds exhibit similar protective effects on myocardial cells (Figure 2B-C, H-I). In addition, immunofluorescence experiments indicate that, compared with the OGD/R group, the treatment with HY and BA significantly enhances the fluorescence expression of SERCA2a in myocardial cells (Figure 2D, E).

Molecular docking and dynamic simulation of HY binding to sarco/endoplasmic reticulum Ca^{2+} receptors

Molecular docking studies revealed that HY interacts with three sarco/endoplasmic reticulum calcium-related proteins—SERCA2a, RYR2, and IP3R—with distinct binding characteristics (Figure 3A). For SERCA2a, the docking showed a binding energy of –4.3 kcal/mol, primarily due to hydrogen bonding with ARG-677 along with hydrophobic contacts. In contrast, HY exhibited weaker binding to RYR2 (–3.2 kcal/mol, involving a hydrogen bond with LEU-9) and IP3R (–3.8 kcal/mol, with hydrogen bonds at THR-268 and ARG-503), which may contribute to modulating calcium release while its key action remains on SERCA2a. When the SERCA2 channel adopts an open conformation, a cavity between Helix 1 and Helix 2 of the pore-forming domain accommodates small molecules. Molecular docking demonstrated that HY binds to this region, suggesting its potential to stabilize the channel's open state (Figure 3B). Molecular dynamics simulations (≥100 ns) confirmed the stability of the HY-SERCA2a complex. Root mean square deviation (RMSD) analysis revealed dynamic equilibrium after 20 ns with minimal structural drift (Figure 3C). The radius of gyration (Rg) indicated preserved global compactness without significant deformation, confirming that HY binding does not disrupt protein folding (Figure 3D). Solvent-accessible surface area (SASA) analysis suggested no substantial alteration in surface exposure, implying HY binding within a hydrophobic cavity (e.g., the Helix1-Helix2 interface) (Figure 3E). Residue-wise root mean square fluctuation (RMSF) showed high flexibility in the calcium-binding domain (residues 200–600), essential for functional activity, while the transmembrane core (residues 800–1000) maintained rigidity to ensure structural stability (Figure 3F). Hydrogen bond analysis revealed persistent interactions between HY and SERCA2a, enhancing binding affinity and interfacial stability (Figure 3G). Collectively, these results indicate that HY stabilizes the open conformation of SERCA2a by occupying the Helix1-Helix2 cavity, forming a stable hydrogen-bonding network to maintain dynamic equilibrium, and likely modulates calcium transport activity through allosteric effects.

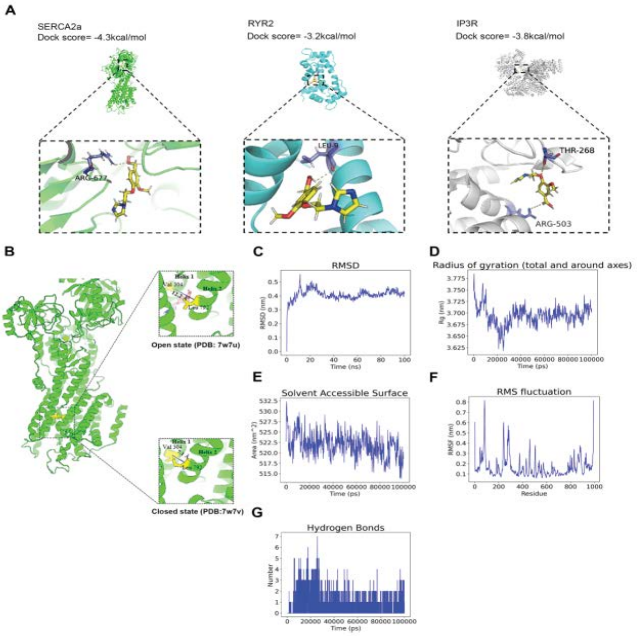

Figure 3: Molecular docking and dynamic simulation of HY binding to sarco/endoplasmic reticulum Ca^{2+} receptors. (A) Molecular docking of HY with SERCA2a, RYR2, and IP3R receptors; (B) Activation mechanism of the HY–SERCA2a complex; (C) RMSD analysis of the HY–SERCA2a complex; (D) Rg analysis of the HY–SERCA2a complex; (E) SASA analysis of the HY–SERCA2a complex; (F) RMSF analysis of the HY–SERCA2a complex; (G) Hydrogen bond variations in the HY– SERCA2a complex.

SERCA2a silencing aggravates calcium overload, ER stress, and mitochondrial damage in myocardial injury

SERCA2a is the primary isoform of the SR calcium pump in cardiac cells, playing a crucial role in regulating intracellular Ca^{2+} concentration, which is essential for both cardiac relaxation and contraction [48-50]. Our study shows that SERCA2a activity is critical for controlling myocardial injury. When SERCA2a was silenced, the OGD/R group exhibited clear disruptions in calcium cycling in cardiac myocytes (Figure 4A), which led to reduced intracellular ATP production (Figure 4D). Under OGD/R conditions in vitro, electron microscopy of AC16 cells revealed severe mitochondrial damage, such as increased fragmentation, disrupted cristae, and loss of the outer membrane (Figure 4E). Further analysis of calcium ion channels and endoplasmic reticulum stress markers confirmed that silencing SERCA2a worsened calcium cycling dysfunction and ER stress compared to the OGD/R group. Treatment with the small molecule HY partly relieved the damage caused by SERCA2a silencing. HY restored SERCA2a protein levels and reduced the expressions of NCX-1, ATF-6, GRP78, and CHOP (Figures 4B-C, F-G). In myocardial infarction, reduced SERCA2a expression contributes to calcium overload, increased p-CREB levels, activation of apoptotic pathways, and worsening of injury.

Citation: Yuqing Chu, Xinya Wang, Hongyan Zhang, Shihao Wan, Qiuju Zhao, Yani Guo, Ke Niu, Binshan Zha, Jiajia Mo, Qichao Luo, Zhaoxing Chu, Liwen Chen, Liuyi Dong. Unveiling the Cardioprotective Potential of HY-021068: Dual Modulation of Calcium Homeostasis and Endoplasmic Reticulum Stress in Myocardial Infarction in Mice. Cardiology and Cardiovascular Medicine.10 (2026): 127-144.

Chu Y, et al., Cardiol Cardiovasc Med 2026
DOI:10.26502/fccm.92920492

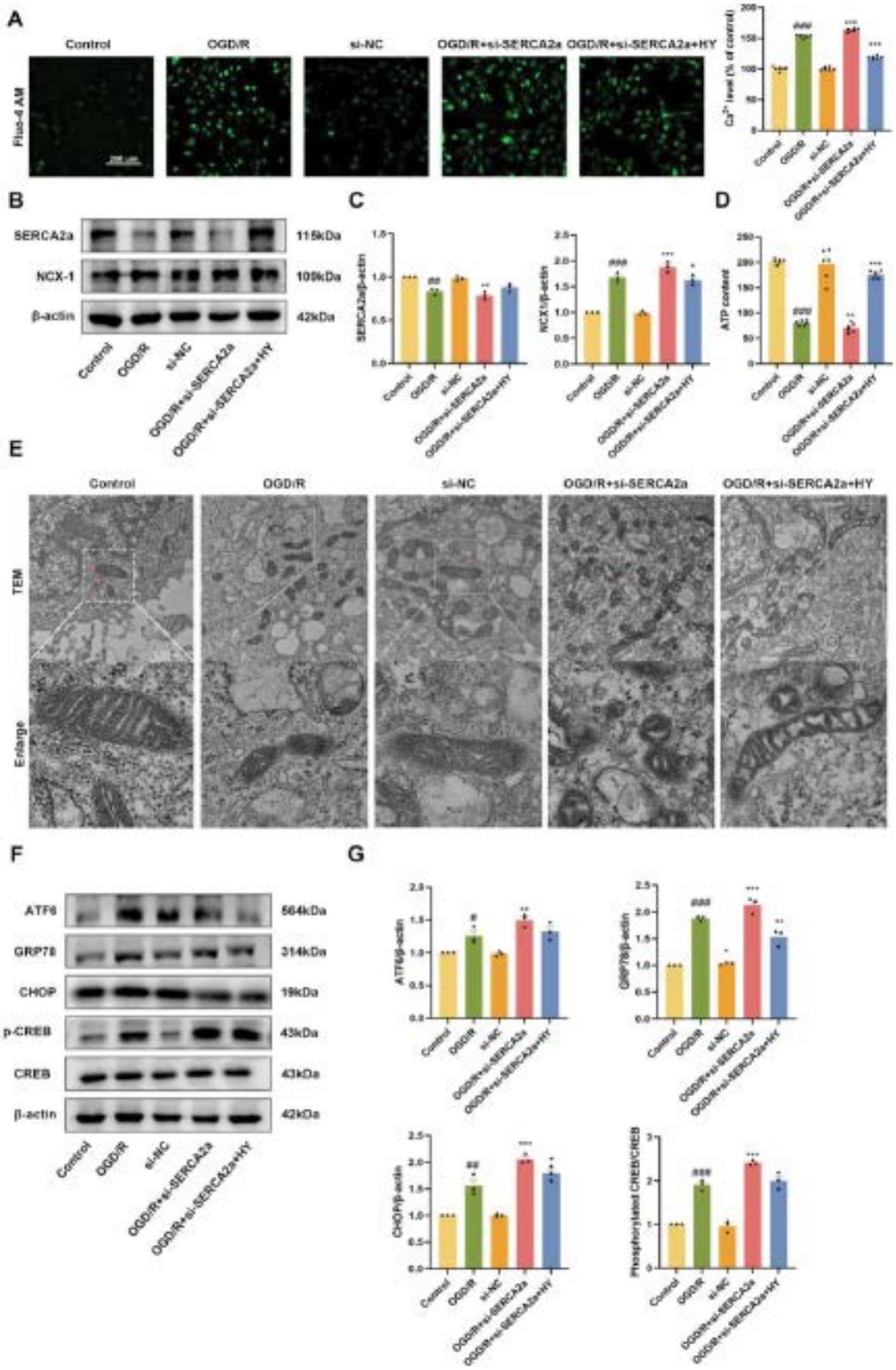

Figure 4: SERCA2a silencing aggravates calcium overload, ER stress, and mitochondrial damage in myocardial injury. (A) ROS fluorescence levels and semi-quantitative analysis, scale bar 200 μm, n=6; (B-C) The expressions of SERCA2a and NCX-1 proteins, n=3; (D) intracellular ATP level, n=6; (E) Representative images of mitochondria in AC16 cells captured at 13,500 × magnification, (n=4); (F-G) ER stress markers (ATF6, GRP78, CHOP) and CREB/p-CREB expression, n=3. $^{\#}P<0.05$ VS Control, $^{\#\#}P<0.01$ VS Control, $^{\#\#\#}P<0.001$ VS Control, $^{*}P<0.05$ VS OGD/R, $^{**}P<0.01$ VS OGD/R, $^{***}P<0.001$ VS OGD/R.

Citation: Yuqing Chu, Xinya Wang, Hongyan Zhang, Shihao Wan, Qiuju Zhao, Yani Guo, Ke Niu, Binshan Zha, Jiajia Mo, Qichao Luo, Zhaoxing Chu, Liwen Chen, Liuyi Dong. Unveiling the Cardioprotective Potential of HY-021068: Dual Modulation of Calcium Homeostasis and Endoplasmic Reticulum Stress in Myocardial Infarction in Mice. Cardiology and Cardiovascular Medicine.10 (2026): 127-144.

Chu Y, et al., Cardiol Cardiovasc Med 2026
DOI:10.26502/fccm.92920492

Notably, silencing SERCA2a raised p-CREB levels, and HY did not counteract this effect, highlighting SERCA2a's key role in regulating CREB phosphorylation. Overall, these results indicate that SERCA2a is crucial in the protective effects of HY against calcium overload-induced myocardial injury by modulating ER stress, mitochondrial damage, and the pro-apoptotic pathway.

SERCA2a overexpression and HY synergistically protect against OGD/R-induced myocardial damage

SERCA2a regulates cardiac contraction and relaxation by transporting Ca^{2+} from the cytoplasm into the SR [51-53]. Enhanced expression of SERCA2a has been shown to improve cardiac contractile performance in myocardial infarction [54-56]. Both the transcriptional and protein levels of SERCA2a fall in cardiac tissue of those with myocardial infarction. This study found that the transfection of the empty plasmid (EV group) had little effect on the cells relative to the OGD/R group. Although the oxidative stress got on by OGD/R was a lot reduced by the SERCA2a overexpression group (SERCA2a-OE group), and also reduced the making at ATP and the potential of the mitochondrial membrane (Figure 5A, B). The overexpression of SERCA2a significantly inhibited the expressions of NCX-1, ATF-6, GRP78, CHOP and p-CERB (Figure 5C-D, F-G). HY further synergistically enhances this effect, indicating that the activity of SERCA2a is negatively correlated with the levels of NCX-1, ATF-6, GRP78, CHOP, and p-CREB. Further, the HY-induced low lipid ROS levels was further aided by the SERCA2a-OE group (Figure 5E). The experimental results showed that the small molecule HY enhanced the protective effect of SERCA2a overexpression against myocardial infarction, indicating that HY can directly regulate the expression of SERCA2a, thereby improving myocardial injury.

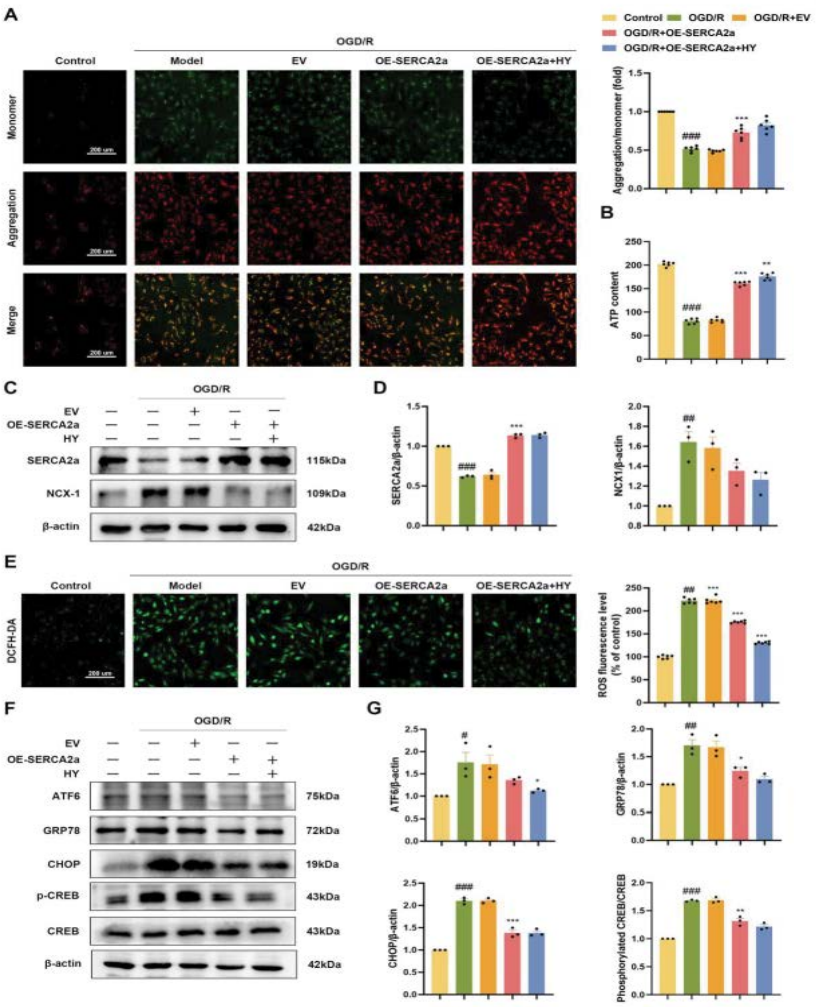

Figure 5: SERCA2a overexpression and HY synergistically protect against OGD/R-induced myocardial damage. (A) Fluorescence levels and semi-quantitative analysis of JC-1, scale bar 200 μm, n=6; (B) ATP levels, n=6; (C-D) The expressions of SERCA2a and NCX-1 proteins, n=3; (E) ROS fluorescence levels and semi-quantitative analysis, scale bar 200 μm, n=6; (F-H) ER stress markers (ATF6, GRP78, CHOP) and CREB/p-CREB expression, n=3. $^{\#}P<0.05$ VS Control, $^{\#\#}P<0.01$ VS Control, $^{\#\#\#}P<0.001$ VS Control, $^{*}P<0.05$ VS OGD/R, $^{**}P<0.01$ VS OGD/R, ***P<0.001 VS OGD/R.

Citation: Yuqing Chu, Xinya Wang, Hongyan Zhang, Shihao Wan, Qiuju Zhao, Yani Guo, Ke Niu, Binshan Zha, Jiajia Mo, Qichao Luo, Zhaoxing Chu, Liwen Chen, Liuyi Dong. Unveiling the Cardioprotective Potential of HY-021068: Dual Modulation of Calcium Homeostasis and Endoplasmic Reticulum Stress in Myocardial Infarction in Mice. Cardiology and Cardiovascular Medicine.10 (2026): 127-144.

Chu Y, et al., Cardiol Cardiovasc Med 2026
DOI:10.26502/fccm.92920492

HY protects against LAD-induced acute myocardial infarction

We made a mouse model of myocardial infarction using the LAD artery ligation means aiming to further study the routine affect of HY against myocardial infarction. The successful establishment of the M/I model was confirmed by a blood flow imager (Figure 6A). To our findings, the M/I group's blood level of LDH and heart weight to body weight ratio (HW/BW) rose relative to the Sham group; though, these increases were significantly reduced following getting HY or clopidogrel therapy (Figure 6B-C). Additionally, we found that compared with the M/I group, administration of HY significantly improved cardiac function, reduced the area of myocardial infarction, alleviated the disordered arrangement of myocardial cells, and decreased myocardial fibrosis, demonstrating that its protective effect against myocardial infarction was comparable to that of clopidogrel (Figure 6D-J).

HY attenuates M/I-induced myocardial calcium overload and ER stress in mice

Thromboxane synthase inhibitors reduce thromboxane (TXA2) synthesis, thereby inhibiting platelet aggregation and vasoconstriction. This improves myocardial blood flow, limits infarct size, alleviates cardiomyocyte injury, and provides significant cardioprotection. TXB_2 and 6-keto-PGF1α are stable metabolites of TXA2 and PGI2, respectively, and their balance is crucial for maintaining normal platelet-vascular interactions. Our results show that both HY and clopidogrel suppressed the M/I-induced increase in TXB2 and platelet aggregation, while preventing the reduction in 6-keto-PGF1α (Figure 7 A, D). In addition, HY and clopidogrel downregulated thromboxane synthesis-related proteins, including TBXAS-1, PGD, and COX-1 (Figure 7B, C). Immunohistochemistry and calcium level measurements further revealed that HY enhanced SERCA2a expression, reduced CHOP levels, and

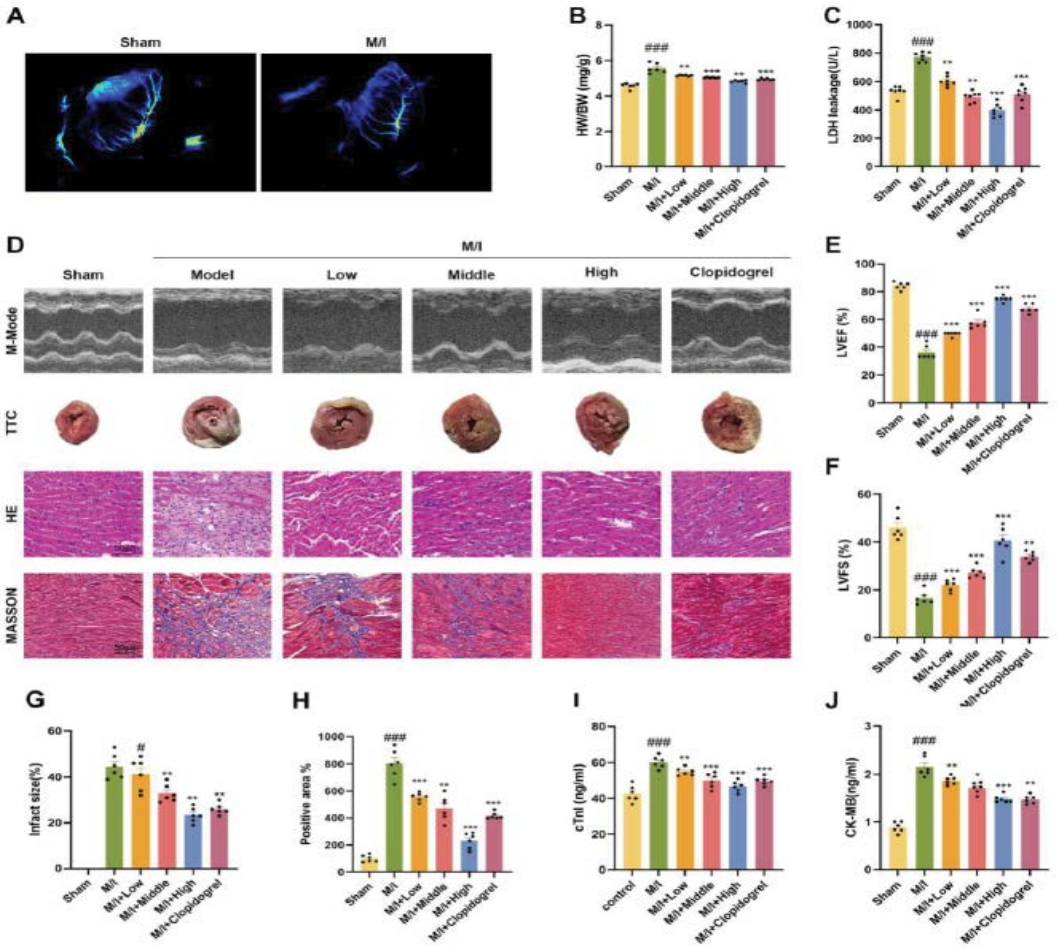

Figure 6: HY protects against LAD-induced acute myocardial infarction. (A) Cardiac blood flow imaging of the hearts of mice in the sham operation control group or the M/I group, n=4; (B) The ratio of the left ventricular heart weight to the body weight (HW/BW) of mice, n=6; (C) The level of LDH in the serum of mice, n=6; (D-H) Results of M-mode echocardiography, TTC staining, HE staining, Masson staining and semi-quantitative analysis of mice, scale bar 50 μm, n=6; (I-J) The levels of cTnI and CK-MB in the serum of mice, n=6. $^{\#}P<0.05$ VS Control, $^{\#\#}P<0.01$ VS Control, $^{\#\#\#}P<0.001$ VS Control, $^{*}P<0.05$ VS OGD/R, $^{**}P<0.01$ VS OGD/R, $^{***}P<0.001$ VS OGD/R.

Citation: Yuqing Chu, Xinya Wang, Hongyan Zhang, Shihao Wan, Qiuju Zhao, Yani Guo, Ke Niu, Binshan Zha, Jiajia Mo, Qichao Luo, Zhaoxing Chu, Liwen Chen, Liuyi Dong. Unveiling the Cardioprotective Potential of HY-021068: Dual Modulation of Calcium Homeostasis and Endoplasmic Reticulum Stress in Myocardial Infarction in Mice. Cardiology and Cardiovascular Medicine.10 (2026): 127-144.

Chu Y, et al., Cardiol Cardiovasc Med 2026
DOI:10.26502/fccm.92920492

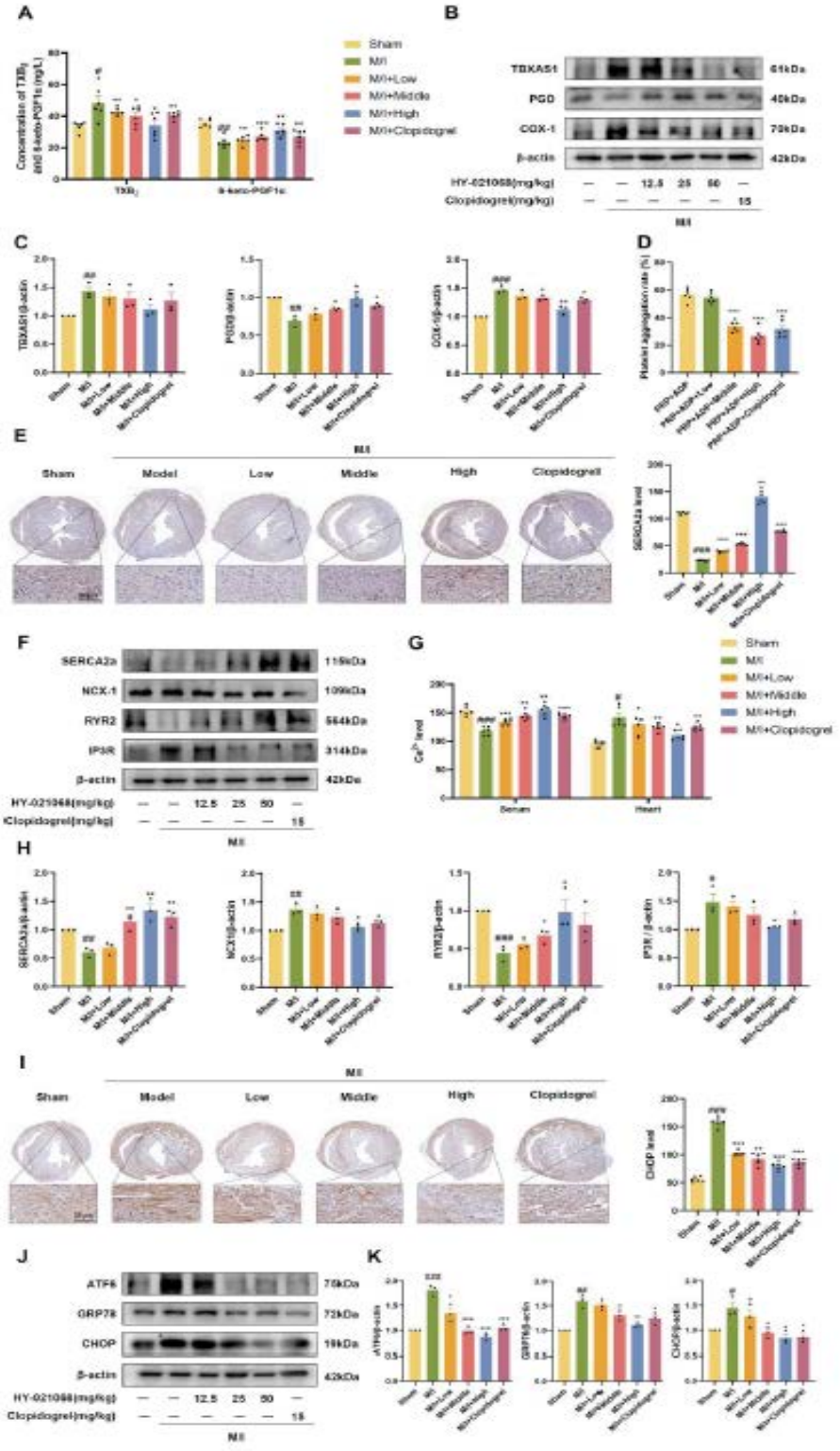

Figure 7: HY attenuates M/I-induced myocardial calcium overload and ER stress in mice. (A) Serum levels of TXB2 and 6-keto-PGF1α in mice, n=6; (B-C) Western blot analysis of TBXAS-1, PGD, and COX-1 expression, n=3; (D) Platelet aggregation rate in mice, n=6; (E) Immunohistochemical analysis of SERCA2a expression in mouse hearts, n=6; (F, H) Western blot analysis of SERCA2a, NCX-1, RYR2, and IP3R, n=3; (G) Ca^{2+} levels in serum and myocardial tissue, n=6; (I) Immunohistochemical analysis of CHOP expression in mouse hearts (n=6); (J-K) Western blot analysis of ATF6, GRP78, and CHOP, n=3. $^{\#}P<0.05$ VS Control, $^{\#\#}P<0.01$ VS Control, $^{\#\#\#}P<0.001$ VS Control, $^{*}P<0.05$ VS OGD/R, $^{**}P<0.01$ VS OGD/R, $^{***}P<0.001$ VS OGD/R.

Citation: Yuqing Chu, Xinya Wang, Hongyan Zhang, Shihao Wan, Qiuju Zhao, Yani Guo, Ke Niu, Binshan Zha, Jiajia Mo, Qichao Luo, Zhaoxing Chu, Liwen Chen, Liuyi Dong. Unveiling the Cardioprotective Potential of HY-021068: Dual Modulation of Calcium Homeostasis and Endoplasmic Reticulum Stress in Myocardial Infarction in Mice. Cardiology and Cardiovascular Medicine.10 (2026): 127-144.

lowered myocardial Ca^{2+} concentration compared to the M/I group, thereby improving calcium cycling and reducing cell death (Figure 7E, I). Protein analysis showed that, in contrast to the Sham group, M/I greatly altered the expression of markers related to calcium and ER stress (IP3R, RYR2, SERCA2a, NCX-1, GRP78, ATF6, and CHOP) (Figure 7F-G, J-K). Treatment with HY (25 or 50 mg/kg) or clopidogrel (25 mg/kg) effectively reversed these changes, indicating that HY restores calcium homeostasis and ER function in the AMI mouse model.

Discussion

In this work, we show that the myocardial contractile function of mice with a myocardial infarction is directly and positively driven by the activation of SERCA2a via HY. Myocardial ischemic necrosis, resulting from obstructed coronary blood flow, leads to reduced SERCA2a activity, which impairs calcium reuptake, decreases SERCA2a-mediated Ca^{2+} transport into the SR, increases NCX1-mediated Ca^{2+} efflux, and induces RYR2 dysfunction, all of which culminate in diastolic calcium leak [50,57,58]. They fall SR calcium levels, avoid contractile and relaxation factors, and ultimately cut the amplitude of myocardial cell shortening. HY mitigates these effects by directly upregulating SERCA2a expression, improving intracellular Ca^{2+} cycling, inhibiting ER stress, and preventing ROS production, thereby enhancing cardiac function.

HY is a thromboxane TXA_2 synthase inhibitor and a novel Class I chemical entity. Previous studies have shown that HY possesses antiplatelet aggregation and antithrombotic properties, providing therapeutic benefits in conditions such as laurate-induced peripheral vascular occlusive vasculitis and ischemic stroke. In the present study, we found that HY treatment highly rebuilt heart activity and improved prognosis after myocardial infarction. Specifically, HY boosted SERCA2a activity, restored calcium homeostasis in myocardial cells, alleviated oxidative stress, and reversed mitochondrial dysfunction, all of which contributed to its cardioprotective effects. Moreover, silencing the SERCA2a gene abolished the cardioprotective effects of HY, resulting in calcium cycling dysregulation and exacerbation of ER stress. In contrast, overexpression of SERCA2a conferred protective effects, suggesting a pivotal role for SERCA2a in mediating HY's therapeutic benefits.

Calcium overload is a central mechanism underlying myocardial damage induced by AMI [59,60]. Under normal physiological conditions, action potentials (APs) propagate along the sarcolemma and T-tubules (TT), activating L-type calcium channels (LTCCs), which allow a small influx of Ca^{2+} [61]. This increase in local Ca^{2+} concentration between the sarcolemma or TT and Junctophilin-2 (JPH2) triggers calcium sparks, which in turn activate the SR to release Ca^{2+} into the cytoplasm via RYR2, resulting in calcium transients [50]. This phenomenon, known as calcium-induced calcium release (CICR), rapidly elevates cytosolic Ca^{2+} concentrations in cardiomyocytes, which leads to muscle contraction through the binding of Ca^{2+} to troponin, inducing conformational changes in actin and myosin filaments [62]. The contractile force generated is proportional to the number of cross-bridges formed, which is influenced by intracellular Ca^{2+} concentration and myocardial cell sensitivity to calcium. In our study, an in vitro model demonstrated that, following OGD/R, Ca^{2+} and ROS levels were significantly elevated in AC16 cells, while extracellular Ca^{2+} and ATP levels were reduced, indicating calcium overload associated with myocardial infarction. BA, a calcium chelator, bound free Ca^{2+}, forming stable calcium complexes and effectively inhibited the rise in Ca^{2+} and ROS levels induced by OGD/R, while reducing ATP production and Ca^{2+} efflux. HY treatment exhibited similar effects, underscoring its role in preventing calcium overload and oxidative stress.

The role of SERCA2a in maintaining calcium homeostasis is well-documented [63,64]. SERCA2a is the primary calcium pump in the SR of cardiac cells, crucial for regulating cytosolic Ca^{2+} concentrations and enabling cardiac relaxation and contraction [20,65-67]. It has been shown that the expression of SERCA2a is regulated by phospholamban (PLN) and phospholamban-like proteins (PLB) [68]. PLN inhibits SERCA2a activity by reducing its affinity for Ca^{2+} [69]. Under low cytosolic Ca^{2+} conditions, PLN interacts with SERCA2a, decreasing its affinity for calcium [70]. Upon increased calcium concentration, Ca^{2+}/calmodulin-dependent protein kinase II (CaMKII) becomes activated, leading to phosphorylation of PLN at Thr-17, which relieves PLN's inhibitory effect on SERCA2a. Additionally, protein kinase A (PKA) phosphorylates PLN at Ser16, diminishing its inhibition of SERCA2a, thus promoting more efficient myocardial relaxation [71,72]. Daniel et al. [73] provided further structural insights into the interaction between PLN and SERCA2a, clarifying their roles in calcium transport. Our findings, however, suggest that silencing the SERCA2a gene significantly reduced SERCA2a immunofluorescence intensity, impaired mitochondrial membrane potential, suppressed ATP production, and reduced intracellular Ca^{2+} efflux, indicating mitochondrial damage in cardiomyocytes. Immunoblotting confirmed that silencing SERCA2a downregulated its activity and upregulated NCX-1 expression. Treatment with HY (40 mm) partially reversed the myocardial damage caused by SERCA2a silencing. This result aligns with previous studies confirming that SERCA2a overexpression is an effective therapeutic strategy for myocardial infarction. Our data also indicate that HY enhances the protective effects of SERCA2a overexpression, suggesting that the compound improves cardiac function by directly modulating SERCA2a expression.

Maintaining ER calcium homeostasis is critical for proper cellular function and Ca^{2+} signaling [74,75]. The ER's calcium balance is regulated by calcium-binding proteins such as calnexin, BiP, and GRP78, along with ER-resident Ca^{2+} transporters and regulators, including RYRs, IP3Rs, and SERCA [76]. It is known that the SERCA inhibitor TG induces ER calcium leakage, leading to depletion of ER Ca^{2+} stores, triggering ER dysfunction, and activating the unfolded protein response (UPR) [77]. The UPR involves three main signaling pathways: the IRE1α pathway (involving GRP78), the PERK pathway (involving CHOP), and the ATF6 pathway [78]. During ER stress, these pathways are activated to mitigate stress and promote cell survival [79]. However, if adaptive UPR feedback is insufficient, UPR signaling remains activated, leading to chronic ER stress, terminal UPR activation, and cell death[80]. Our study demonstrates that HY-021068 inhibited the activity of ATF6, GRP78, and CHOP proteins, thus mitigating ER stress-induced damage in the myocardium following OGD/R and LAD surgery.

Conclusions

In summary, our study suggests HY rises SERCA2a activity, preserving the heart in myocardial infarction. This mechanism mitigates calcium overload induced by infarction, alleviates ER stress, prevents mitochondrial damage, and suppresses pro-apoptotic pathways. These findings provide novel insights into the cardioprotective mechanisms of HY, highlighting its potential as a multi-target therapeutic agent for ischemic heart disease.

Graphical Abstract

Schematic diagram of the mechanism by which HY inhibits calcium overload to prevent acute myocardial infarction injury. HY upregulates SERCA2a to stabilize the calcium pump, restore myocardial calcium homeostasis, inhibit oxidative/ER stress, thereby preventing calcium overload and alleviating acute myocardial infarction injury.

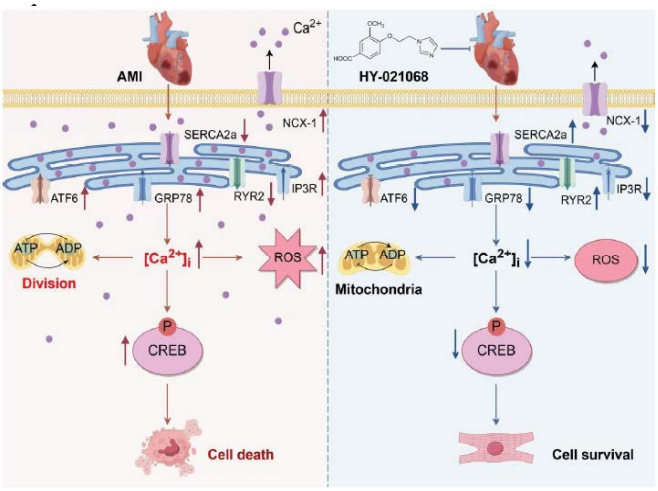

Funding

This study was supported by Anhui Provincial Natural Science Foundation (2108085MH254), Anhui Provincial Key Research and Development Program (202303a07020009), and Basic and Clinical Cooperative Research and Promotion Program of Anhui Medical University (2021xkjT028).

Author contributions

Yuqing Chu, Xinya Wang: writing—original draft, methodology, experimental manipulation. Hongyan Zhang: validation. Shihao Wan: formal analysis, software. Yani Guo: visualization. Ke Niu: resources, investigation. Binshan Zha: Data curation. Jiajia Mo: Project administration. Qichao Luo: Supervision. Zhaoxing Chu: Project administration. Liwen Chen: Supervised experiments. Liuyi Dong: designed the study, supervision, funding acquisition.

Data Availability

The data supporting the results of this study are archived at Anhui Medical University and are backed up at the Department of Pharmacology. Access to the data may be granted upon reasonable request.

Conflicts of Interest

The authors have no conflicts of interest regarding this manuscript.

Acknowledgments

The authors wish to acknowledge the invaluable support and contributions of all collaborators to this study. Special thanks are extended to the members of the Center for Scientific Research of Anhui Medical University for their technical support and guidance during the experiments.

References

1. Abbate A, Toldo S, Marchetti C, et al. Interleukin-1 and the Inflammasome as Therapeutic Targets in Cardiovascular Disease [J]. Circulation Research 126 (2020): 1260-80.
2. Ainiwaer A, Kadier K, Abulizi A, et al. Association of red cell distribution width (RDW) and the RDW to platelet count ratio with cardiovascular disease among US adults: a cross-sectional study based on the National Health and Nutrition Examination Survey 1999-2020 [J]. BMJ Open 13 (2023): e068148.
3. Tian X, Liu P, Wang R, et al. A review on the treatment of hyperlipidemia with Erchen Decoction [J]. Frontiers in Pharmacology 15 (2024): 1445950.
4. Deng Q, Li X X, Fang Y, et al. Therapeutic Potential of Quercetin as an Antiatherosclerotic Agent in Atherosclerotic Cardiovascular Disease: A Review [J]. Evidence-Based Complementary and Alternative Medicine: eCAM (2020): 5926381.

5. Wang J, Xu R, Wu J, et al. MicroRNA-137 Negatively Regulates H_2O_2-Induced Cardiomyocyte Apoptosis Through CDC42 [J]. Medical science monitor: International Medical Journal of Experimental and Clinical Research 21 (2015): 3498-504.
6. Zhang Z, Feng HZ, Jin JP. Structure of the NH2-terminal variable region of cardiac troponin T determines its sensitivity to restrictive cleavage in pathophysiological adaptation [J]. Archives of Biochemistry and Biophysics 515 (2011): 37-45.
7. Cao X, Wei M, Tang M, et al. Acute Myocardial Infarction and Concomitant Acute Intracranial Hemorrhage: Clinical Characteristics and Outcomes [J]. Journal of Investigative Medicine: the official publication of the American Federation for Clinical Research 70 (2022): 1713-9.
8. Liu LK, Ouyang W, Zhao X, et al. Pathogenesis and Prevention of Radiation-induced Myocardial Fibrosis [J]. Asian Pacific Journal of Cancer Prevention : APJCP 18 (2017): 583-7.
9. He J, Fu L H, Qi C, et al. Metal peroxides for cancer treatment [J]. Bioactive Materials 6 (2021): 2698-710.
10. Lei H, Pei Z, Jiang C, et al. Recent progress of metal-based nanomaterials with anti-tumor biological effects for enhanced cancer therapy [J]. Exploration (Beijing, China) 3 (2023): 20220001.
11. Liu Y, Zhang J, Zhang D, et al. Research Progress on the Role of Pyroptosis in Myocardial Ischemia-Reperfusion Injury [J]. Cells 11 (2022).
12. Pagliaro P, Penna C. Inhibitors of NLRP3 Inflammasome in Ischemic Heart Disease: Focus on Functional and Redox Aspects [J]. Antioxidants (Basel, Switzerland) 12 (2023).
13. Lai Y, Gao FF, Ge RT, et al. Metal ions overloading and cell death [J]. Cell Biology and Toxicology 40 (2024): 72.714.
14. Oliveira MA, Brandi AC, Dos Santos CA, et al. The calcium paradox - what should we have to fear? [J]. Revista brasileira de cirurgia cardiovascular : orgao oficial da Sociedade Brasileira de Cirurgia Cardiovascular 29 (2014): 249-54.
15. Kim Y, Ko T H, Jin C, et al. The emerging roles of Shank3 in cardiac function and dysfunction [J]. Frontiers in cell and Developmental Biology 11 (2023): 1191369.
16. Zhang J, Shi X, Gao J, et al. Danhong Injection and Trimetazidine Protect Cardiomyocytes and Enhance Calcium Handling after Myocardial Infarction [J]. Evidence-based complementary and alternative medicine: eCAM (2021): 2480465.
17. Fang H, Yang L, Yan M, et al. Research progress in cardiotoxicity of organophosphate esters [J]. Frontiers in Pharmacology 14 (2023): 727.
18. Retraction: Overexpression of SERCA2a alleviates cardiac microvascular ischemic injury by suppressing Mfn2-mediated ER/mitochondrial calcium tethering [J]. Frontiers in Cell and Developmental Biology 10 (2022): 1006540.
19. Hu Y, Zhang C, Zhu H, et al. Luteolin modulates SERCA2a via Sp1 upregulation to attenuate myocardial ischemia/reperfusion injury in mice [J]. Scientific reports 10 (2020): 15407.
20. Oldfield C J, Moffatt T L, O'hara K A, et al. Muscle-specific sirtuin 3 overexpression does not attenuate the pathological effects of high-fat/high-sucrose feeding but does enhance cardiac SERCA2a activity [J]. Physiological Reports 9 (2021): e14961.
21. Cleary SR, Fang X, Cho EE, et al. Inhibitory and stimulatory micropeptides preferentially bind to different conformations of the cardiac calcium pump [J]. The Journal of Biological Chemistry 298 (2022): 102060.
22. Oneglia A, Nelson MD, Merz C NB. Sex Differences in Cardiovascular Aging and Heart Failure [J]. Current Heart Failure Reports 17 (2020): 409-23.
23. Wang Z, Zhang Y, Wang L, et al. NBP Relieves Cardiac Injury and Reduce Oxidative Stress and Cell Apoptosis in Heart Failure Mice by Activating Nrf2/HO-1/Ca(2+)-SERCA2a Axis [J]. Evidence-Based Complementary and Alternative Medicine : eCAM (2022): 7464893.
24. Kho C, Lee A, Jeong D, et al. Small-molecule activation of SERCA2a SUMOylation for the treatment of heart failure [J]. Nature Communications 6 (2015): 7229.
25. Gorski PA, Lee A, Lee P, et al. Identification and Characterization of p300-Mediated Lysine Residues in Cardiac SERCA2a [J]. International Journal of Molecular Sciences 24 (2023).
26. Liu H, Liu W, Qiu H, et al. Salvianolic acid B protects against myocardial ischaemia-reperfusion injury in rats via inhibiting high mobility group box 1 protein expression through the PI3K/Akt signalling pathway [J]. Naunyn-Schmiedeberg's Archives of Pharmacology 393 (2020): 1527-39.
27. Shi J, Wei L. Rho kinases in cardiovascular physiology and pathophysiology: the effect of fasudil [J]. Journal of Cardiovascular Pharmacology 62 (2013): 341-54.
28. Xiong L, Cao J, Qiu Y, et al. Exploring the Mechanism of Aspirin in the Treatment of Kawasaki Disease Based on Molecular Docking and Molecular Dynamics

[J]. Evidence-based Complementary and Alternative Medicine: eCAM (2022):

29. Li P, Huang J, Geng D, et al. Semi-Mechanistic Modeling of HY-021068 Based on Irreversible Inhibition of Thromboxane Synthetase [J]. Frontiers in Pharmacology 11 (2020): 588286.
30. Chang X, Yao S, Wu Q, et al. Tongyang Huoxue Decoction (TYHX) Ameliorating Hypoxia/Reoxygenation-Induced Disequilibrium of Calcium Homeostasis and Redox Imbalance via Regulating Mitochondrial Quality Control in Sinoatrial Node Cells [J]. Oxidative Medicine and Cellular Longevity (2021): 3154501.
31. Greenberg B. Medical Management of Patients with Heart Failure and Reduced Ejection Fraction [J]. Korean Circulation Journal 52 (2022): 173-97.
32. Brown DI, Cooley BC, Quintana MT, et al. Nebulized Delivery of the MAPKAP Kinase 2 Peptide Inhibitor MMI-0100 Protects Against Ischemia-Induced Systolic Dysfunction [J]. International Journal of Peptide Research and Therapeutics 22 (2016): 317-24.
33. Lu D, Liao Y, Zhu SH, et al. Bone-derived Nestin-positive mesenchymal stem cells improve cardiac function via recruiting cardiac endothelial cells after myocardial infarction [J]. Stem Cell Research & Therapy 10 (2019): 127.
34. Polzin A, Dannenberg L, Benkhoff M, et al. Sphingosine-1-phosphate improves outcome of no-reflow acute myocardial infarction via sphingosine-1-phosphate receptor 1 [J]. ESC Heart Failure 10 (2023): 334-41.
35. Bao YR, Jiang WY, Yu JY, et al. Traditional Chinese Medicine Formulation Huangqi Jianzhong Tang Improves Cardiac Function after Myocardial Infarction in Rats [J]. Evidence-based Complementary and Alternative Medicine : eCAM (2020): 3106076.
36. Jo W, Min BS, Yang HY, et al. Sappanone A Prevents Left Ventricular Dysfunction in a Rat Myocardial Ischemia Reperfusion Injury Model [J]. International Journal of Molecular Sciences 21(2020).
37. Szabó R, Karácsonyi Z, Börzsei D, et al. Role of Exercise-Induced Cardiac Remodeling in Ovariectomized Female Rats [J]. Oxidative Medicine and Cellular Longevity (2018): 6709742.
38. Albadawy R, Hasanin AH, Agwa SHA, et al. Rosavin Ameliorates Hepatic Inflammation and Fibrosis in the NASH Rat Model via Targeting Hepatic Cell Death [J]. International Journal of Molecular Sciences 23 (2022).
39. Brzoska T, Suzuki Y, Mogami H, et al. Binding of thrombin-activated platelets to a fibrin scaffold through $\alpha(IIb)\beta_3$ evokes phosphatidylserine exposure on their cell surface [J]. PloS One 8 (2013): e55466.
40. Panova-Noeva M, Wagner B, Nagler M, et al. Comprehensive platelet phenotyping supports the role of platelets in the pathogenesis of acute venous thromboembolism – results from clinical observation studies [J]. EBioMedicine 60 (2020): 102978.
41. Maloney J P, Narasimhan J, Biller J. Decreased TGF-β1 and VEGF Release in Cystic Fibrosis Platelets: Further Evidence for Platelet Defects in Cystic Fibrosis [J]. Lung 194 (2016): 791-8.
42. Stevens SA, Sunilkumar S, Subrahmanian SM, et al. REDD1 Deletion Suppresses NF-κB Signaling in Cardiomyocytes and Prevents Deficits in Cardiac Function in Diabetic Mice [J]. International Journal of Molecular Sciences 25 (2024).
43. Xu Z, Wang S, Ji H, et al. Broccoli sprout extract prevents diabetic cardiomyopathy via Nrf2 activation in db/db T2DM mice [J]. Scientific Reports 6 (2016): 30252.
44. Huang R, Zhang C, Wang X, et al. PPARγ in Ischemia-Reperfusion Injury: Overview of the Biology and Therapy [J]. Frontiers in Pharmacology 12 (2021): 600618.
45. Li H, Qiu J, Liu C, et al. MicroRNA-221 protects myocardial contractility in myocardial ischemia/reperfusion injury through phospholamban [J]. PloS one 20 (2025): e0316887.
46. Kim HN, Mccrea MR, Li S. Advances in molecular therapies for targeting pathophysiology in spinal cord injury [J]. Expert Opinion on Therapeutic Targets 27 (2023): 171-87.
47. Gao G, Yu Z, Yan J, et al. Poly (ADP-ribose) polymerase-and cytochrome c-mediated apoptosis induces hepatocyte injury in a rat model of hyperammonia-induced hepatic failure. Molecular Medicine Reports 11 (2015): 4211-9.
48. Liu L, Zhao W, Liu J, et al. Epigallocatechin-3 gallate prevents pressure overload-induced heart failure by up-regulating SERCA2a via histone acetylation modification in mice [J]. PloS one 13 (2018): e0205123.
49. Xu K, Chen C, Wu Y, et al. Advances in miR-132-Based Biomarker and Therapeutic Potential in the Cardiovascular System [J]. Frontiers in Pharmacology 12 (2021): 751487.
50. Yang L, Deng J, Ma W, et al. Ablation of lncRNA Miat attenuates pathological hypertrophy and heart failure [J]. Theranostics 11 (2021): 7995-8007.
51. HIGO S. Disease modeling of desmosome-related cardiomyopathy using induced pluripotent stem cell-derived cardiomyocytes [J]. World Journal of Stem Cells 15 (2023): 71-82.

52. Choi H M, Park M S, Youn J C. Update on heart failure management and future direction [J]. The Korean Journal of Internal Medicine 34 (2019): 944.

53. Zhang R, Ren Y, Ju Y, et al. FAM20C: A key protein kinase in multiple diseases [J]. Genes & Diseases 12 (2025): 101179.

54. Goerg J, Sommerfeld M, Greiner B, et al. Low-Dose Empagliflozin Improves Systolic Heart Function after Myocardial Infarction in Rats: Regulation of MMP9, NHE1, and SERCA2a [J]. International Journal of Molecular Sciences 22 (2021).

55. Gong H, Li Y, Wang L, et al. Short-term effects of β2-AR blocker ICI 118,551 on sarcoplasmic reticulum SERCA2a and cardiac function of rats with heart failure [J]. Experimental and Therapeutic Medicine 12 (2016): 1355-62.

56. Fan S, Hu Y. Role of m6A Methylation in the Occurrence and Development of Heart Failure [J]. Frontiers in Cardiovascular Medicine 9 (2022): 892113.

57. Paterek A, Oknińska M, Mączewski M, et al. Right Ventricle Remodelling in Left-Sided Heart Failure in Rats: The Role of Calcium Signalling [J]. Biomolecules 12 (2022).

58. Monteiro LM, Vasques-Nóvoa F, Ferreira L, et al. Restoring heart function and electrical integrity: closing the circuit [J]. NPJ Regenerative Medicine 2 (2017): 9.

59. Ling X, Lin C, Liu J, et al. Prognostic value of the prognostic nutritional index for patients with acute myocardial infarction undergoing percutaneous coronary intervention with variable glucose metabolism statuses: a retrospective cohort study [J]. Diabetology & Metabolic Syndrome 15 (2023): 207.

60. Lu P, Qi Y, Li X, et al. PEDF and 34-mer peptide inhibit cardiac microvascular endothelial cell ferroptosis via Nrf2/HO-1 signalling in myocardial ischemia-reperfusion injury [J]. Journal of Cellular and Molecular Medicine 28 (2024): e18558.

61. Pölönen RP, PENTTINEN K, SWAN H, et al. Antiarrhythmic Effects of Carvedilol and Flecainide in Cardiomyocytes Derived from Catecholaminergic Polymorphic Ventricular Tachycardia Patients [J]. Stem Cells International (2018): 9109503.

62. Beckendorf J, Van Den Hoogenhof MMG, Backs J. Physiological and unappreciated roles of CaMKII in the heart [J]. Basic Research in Cardiology 113 (2018): 29.

63. Hu S Y, Zhang Y, Zhu P J, et al. Liraglutide directly protects cardiomyocytes against reperfusion injury possibly via modulation of intracellular calcium homeostasis [J]. Journal of Geriatric Cardiology: JGC 14 (2017): 57-66.

64. Hu S, Zhu P, Zhou H, et al. Melatonin-Induced Protective Effects on Cardiomyocytes Against Reperfusion Injury Partly Through Modulation of IP3R and SERCA2a Via Activation of ERK1 [J]. Arquivos Brasileiros de Cardiologia 110 (2018): 44-51.

65. Li A, Yuen SL, Stroik DR, et al. The transmembrane peptide DWORF activates SERCA2a via dual mechanisms [J]. The Journal of Biological Chemistry 296 (2021): 100412.

66. Quick AP, Landstrom AP, Wehrens XH. Junctophilin-2 at the intersection of arrhythmia and pathologic cardiac remodeling [J]. Heart Rhythm 13 (2016): 753-4.

67. Li S, Han R. Targeting miR-25 to alleviate DMD-related muscle dysfunction [J]. Molecular Therapy Nucleic Acids 35 (2024): 102238.

68. Stroik DR, Ceholski DK, Bidwell PA, et al. Viral expression of a SERCA2a-activating PLB mutant improves calcium cycling and synchronicity in dilated cardiomyopathic hiPSC-CMs [J]. Journalof Molecular and Cellular Cardiology 138 (2020): 59-65.

69. Rapti K, Chaanine AH, Hajjar RJ. Targeted gene therapy for the treatment of heart failure [J]. The Canadian Journal of Cardiology 27 (2011): 265-83.

70. Fisher Me, Bovo E, Aguayo-Ortiz R, et al. Dwarf open reading frame (DWORF) is a direct activator of the sarcoplasmic reticulum calcium pump SERCA [J]. eLife 10 (2021).

71. MATTIAZZI A, KRANIAS E G. The role of CaMKII regulation of phospholamban activity in heart disease [J]. Frontiers in Pharmacology 5 (2014): 5.

72. Pastore A, Piemonte F. Protein glutathionylation in cardiovascular diseases [J]. International Journal Of Molecular Sciences 14 (2013): 20845-76.

73. Weber DK, Reddy UV, Wang S, et al. Structural basis for allosteric control of the SERCA-Phospholamban membrane complex by Ca(2+) and phosphorylation [J]. eLife 10 (2021).

74. Xie Y, Wu N, Tang S, et al. Endoplasmic Reticulum Dysfunction: An Emerging Mechanism of Vitiligo Pathogenesis [J]. Clinical, Cosmetic and Investigational Dermatology 17 (2024): 1133-44.

75. Liu Z, Gu S, Lu T, et al. IFI6 depletion inhibits esophageal squamous cell carcinoma progression through reactive oxygen species accumulation via mitochondrial dysfunction and endoplasmic reticulum stress [J]. Journal of Experimental & Clinical Cancer Research: CR 39 (2020): 144.

76. Xu L, Wang X, Tong C. Endoplasmic Reticulum-Mitochondria Contact Sites and Neurodegeneration [J]. Frontiers in Cell and Developmental Biology 8 (2020): 428.

77. OH BC. Phosphoinositides and intracellular calcium signaling: novel insights into phosphoinositides and calcium coupling as negative regulators of cellular signaling [J]. Experimental & Molecular Medicine 55 (2023): 1702-12.

78. Jiang Y, Jiao Y, Liu Y, et al. Sinomenine Hydrochloride Inhibits the Metastasis of Human Glioblastoma Cells by Suppressing the Expression of Matrix Metalloproteinase-2/-9 and Reversing the Endogenous and Exogenous Epithelial-Mesenchymal Transition [J]. International Journal of Molecular Sciences 19 (2018).

79. Vatakuti S, Olinga P, Pennings J L A, et al. Validation of precision-cut liver slices to study drug-induced cholestasis: a transcriptomics approach [J]. Archives of Toxicology 91 (2017): 1401-12.

80. YANG ML, Sodré FMC, MAMULA MJ, et al. Citrullination and PAD Enzyme Biology in Type 1 Diabetes -Regulators of Inflammation, Autoimmunity, and Pathology [J]. Frontiers in Immunology 12 (2021): 678953.

Citation: Yuqing Chu, Xinya Wang, Hongyan Zhang, Shihao Wan, Qiuju Zhao, Yani Guo, Ke Niu, Binshan Zha, Jiajia Mo, Qichao Luo, Zhaoxing Chu, Liwen Chen, Liuyi Dong. Unveiling the Cardioprotective Potential of HY-021068: Dual Modulation of Calcium Homeostasis and Endoplasmic Reticulum Stress in Myocardial Infarction in Mice. Cardiology and Cardiovascular Medicine.10 (2026): 127-144.